Protonation Thermochemistry of α,ω-Alkane Diols in the Gas Phase: A Theoretical Study

G. Bouchoux*,† and F. Berruyer-Penaud‡

Laboratoire des Mécanismes Réactionnels, UMR CNRS 7651, Ecole Polytechnique, 91128 Palaiseau Cedex, France, and Laboratoire de Chimie Physique, Groupe de Chimie Théorique, UMR CNRS 8000, Bâtiment 490, Université Paris-Sud, 91405 Orsay Cedex, France

Received: May 8, 2003; In Final Form: July 16, 2003

The proton affinities of 1,2-ethane diol (**1**), 1,3-propane diol (**2**), and 1,4-butane diol (**3**) were calculated by ab initio molecular orbital calculations at the G2(MP2) level. The values (PA(**1**) = 795.3, PA(**2**) = 851.5, and PA(**3**) = 882.4 kJ·mol^{-1}) are in agreement with recent determinations using the kinetic method but at variance with previous results obtained from equilibrium constant measurements. Entropy differences, $\Delta_pS°(M) = S°(MH^+) - S°(M)$ (M = **1**−**3**), were estimated by explicitly considering the rotational barriers of the torsional modes in both the neutral and the protonated molecules, M. Absolute values of calculated $\Delta_pS°$ (−5, −22, and −32 J·mol^{-1}·K^{-1} for M = **1**, **2**, and **3**, respectively) are lower than that presently available in the literature. Combining the calculated PA(M) and $\Delta_pS°(M)$ leads to gas-phase basicities GB(M) equal to 761.4, 812.4, and 840.4 kJ·mol^{-1} for M = **1**, **2**, and **3**, respectively.

Introduction

Gas-phase protonation energetics of bidentate bases are information of fundamental interest particularly because of their sensitivity to the existence of intramolecular hydrogen bonding in the neutral molecule and in its protonated form. From this point of view, diols are molecules of choice because they are involved in various chemical and biochemical processes. During the last years, the first members of the series of α,ω-alkane diols, 1,2-ethane diol (**1**), 1,3-propane diol (**2**), and 1,4-butane diol (**3**), have been experimentally studied.[1−5] A clear enhancement of the gas-phase basicities of these molecules, with respect to primary alcohols of comparable polarizability, is observed. This is readily explained by the formation of a strong internal hydrogen bond in the protonated forms of the diols, a proposal that has been corroborated by the observation of an entropy loss upon protonation.[1] However, if the experimental results qualitatively agree, surprisingly large differences are to be noted between data obtained using the equilibrium method[1] and the kinetic method[2−5] of determination of gas-phase protonation energetics. Differences between the proton affinity values obtained by the two procedures are as large as 17−34 kJ·mol^{-1}; conflicting results are also obtained for protonation entropies. To identify the origin of these discrepancies, we decided to investigate **1**−**3** and their protonated forms with the help of high-level molecular orbital calculations. Accordingly, it is now established that combined methods such as G2 and their variants provide heats of formation and proton affinities values within an accuracy of ±5 kJ·mol^{-1}.[6] We thus examine neutral and protonated molecules M = **1**−**3** using the G2(MP2) method to obtain theoretical estimates of heats of formation, $\Delta_fH°(M)$ and $\Delta_fH°(MH^+)$, and proton affinities, PA(M). Second, calculation of the protonation entropies, that is, differences $\Delta_pS°(M) = S°(MH^+) - S°(M)$, has been done after considering explicitly the rotational barriers associated with the torsional modes. This procedure has been shown previously to correct the usual approach, which uses the harmonic oscillator approximation and consequently leads to underestimated $S°$ values.[7−9]

Computational Section

Standard ab initio calculations have been carried out using the Gaussian 98 series of programs.[10] Heats of formation have been evaluated from the G2(MP2) total energies by considering the atomization reactions.[11] With the use of this approach, the heat of formation at 0 K for a given species X, $\Delta_fH°_0(X)$, is given by

$$\Delta_fH°_0(X) = \sum\Delta_fH°_0(\text{atoms}) - \sum E[\text{G2(MP2)}](\text{atoms}) + E[\text{G2(MP2)}](X) \quad (1)$$

The heat of formation at 298 K is therefore given by

$$\Delta_fH°_{298}(X) = \Delta_fH°_0(X) + \Delta_{298}H°(X) - \sum\Delta_{298}H°(\text{elements}) \quad (2)$$

where the difference between the enthalpy at 298 K and that at 0 K is represented by the terms $\Delta_{298}H°$ ($\Delta_{298}H° = H°_{298} - H°_0$). For the elements, experimental $\Delta_{298}H°$ values have been used (i.e., 8.468, 1.050, and 8.68 kJ·mol^{-1} for H_2(g), C(s), and O_2(g), respectively), whereas, for the other species, the translational and rotational contributions were taken equal to 3*RT* and the vibrational contribution was estimated from the scaled (by a factor 0.8929) HF/6-31G(d) vibrational frequencies, except for the internal rotations as described below.

The calculation of absolute third-law entropies uses standard statistical thermodynamic formulas.[7] Each vibrational contribution to entropy was computed according to the standard equation

$$S° = R[(\theta/T)/(e^{\theta/T} - 1) - \ln(1 - e^{-\theta/T})] \quad (3)$$

where $\theta = h\nu/k_B$, where h and k_B are the Planck's and

* To whom correspondence should be addressed. Phone: (33) 1 69 33 34 00. E-mail: bouchoux@dcmr.polytechnique.fr.
† Ecole Polytechnique.
‡ Université Paris-Sud.

10.1021/jp030595v CCC: $25.00
Published on Web 09/04/2003

Boltzman's constants, respectively, and using the scaled harmonic vibrational frequencies ν calculated at the HF/6-31G(d) level. Entropies for internal rotations were computed by using the hindered rotor model. In this approach, the energy levels of a rotor associated with a potential energy barrier of the form $(V_0/2)(1 - \cos n\phi)$, where ϕ is the dihedral angle, are found with the help of a one-dimensional Schrödinger equation. Calculations were done by exact solving of the Schrödinger equation[12] and in the frame of the model developed by Pitzer.[13] In this latter case, the entropy of a given rotor is obtained by addition of a corrective term to the entropy calculated under the free rotor approximation, S°_{fr}:

$$S^\circ_{fr} = {}^1/_2 R \ln[8\pi^3 e I_{red} k_B T/(n^2 h^2)] \quad (4)$$

where $e = 2.718\,28$ and I_{red} is the reduced moment of inertia of the two rotating groups around the axis containing the twisting bond. When the energy barrier V_0 is significantly higher than RT, it is generally observed that the harmonic oscillator model reasonably works if the harmonic vibrational frequencies of the torsional modes are calculated using the relationship

$$\nu = (n/(2\pi))(V_0/(2I_{red}))^{1/2} \quad (5)$$

In the present study, the required rotational potential energy barriers, V_0, were obtained at the HF/6-31G(d) level using a relaxed rotation approach without symmetry constraint (i.e., all geometrical parameters were optimized except the dihedral angle considered). A complete scan of the dihedral angle, between 0 and 360° by steps of 5°, was explored for each torsional mode. The global internal rotation potential so obtained is invariably the sum of several cosine potentials. The V_0 values used in the entropy calculations were equated with the difference between maxima and minima of the smoothed potential energy curves. The rotation of asymmetric rotors generates nonequivalent conformations corresponding to various minima of the potential energy curve $V_0(\phi)$. The total entropy of such a mixture of conformers may be determined according to expression 6, where x_i represents the molar fractions of conformer i:

$$S^\circ = \sum x_i S^\circ_i - R\sum x_i \ln x_i \quad (6)$$

If the energy differences between conformers are small, the entropy of mixing, $-R\sum x_i \ln x_i$, may be approximated by $R \ln n_c$, where n_c is the total number of conformers. Thus the correction for mixing exactly compensates for the degeneracy of the rotors, which is accounted for by the factor n in expressions 4 or 5. For the conformers considered, the S°_i terms should be similar because the internal rotations do not produce considerable changes in the principal moments of inertia or in the vibrational frequencies. We thus consider that the term $\sum x_i\ S^\circ_i$ may be equated with the S° of the most stable conformation.

The detailed geometries and vibrational frequencies used in the present work are available as Supporting Information.

Results and Discussion

The presently available experimental protonation energetics data of diols **1**−**3** are summarized in Table 1. In an earlier study of the gas-phase basicity of 1,2-ethane diol, **1**, using a Fourier transform ion cyclotron resonance mass spectrometer, we observed that **1** was able to abstract a proton from $[CH_2{=}CHCHOH]^+$ and $[CH_2{=}C(CH_3)CHOH]^+$ but not from $[(CH_3)_2COH]^+$.[2] Considering the gas-phase basicity values of the concerned molecules,[14] this means that GB(**1**) is less than 780 kJ·mol^{-1} and probably lies in the range 770 ± 10 kJ·mol^{-1}. Chen and Stone[1] used high-pressure mass spectrometry, which allows measurement of the equilibrium constant for proton-transfer reactions over a range of temperatures, to obtain GB(**1**) but also the corresponding proton affinity, PA(**1**), and the protonation entropy, $\Delta_pS^\circ(\mathbf{1}) = S^\circ(\mathbf{1H}^+) - S^\circ(\mathbf{1})$. Several difficulties were encountered by the authors during their experiments; it was found in particular that **1** possesses a high propensity to form proton-bound dimers and $\mathbf{1H}^+$ invariably gives rise to a significant water loss, so the system generally evolves toward a steady state rather than an equilibrium state. For these reasons, only one proton-transfer reaction involving **1** and toluene, as reference base, was studied in the limited 600−530 K range. Assuming that the ΔS° and ΔH° determined from the van't Hoff plot are identical to ΔS°_{298} and ΔH°_{298} and using GB(toluene) = 756.3 kJ·mol^{-1} and Δ_pS°(toluene) = 16 J·mol^{-1}·K^{-1},[14] the following estimates are obtained: GB(**1**) = 774.3 ± 3.1 kJ·mol^{-1}, PA(**1**) = 817.0 ± 2.9 kJ·mol^{-1}, and $\Delta_pS^\circ(\mathbf{1}) = -34.6 \pm 0.8$ J·mol^{-1}·K^{-1}. More recently, we determined the proton affinity of 1,2-ethane diol, **1**, by using the kinetic method in its so-called full entropy analysis extension. Proton-bound heterodimers involving **1** and various reference bases B_i were produced either under chemical ionization conditions[3] or by electrospray ionization.[5] Proton affinity values coming from both experiments (Table 1) show a difference of ca. 15 kJ·mol^{-1} with respect to that obtained by the equilibrium method. More dramatic is the deviation observed between the various estimates of the protonation entropy because the kinetic method detects essentially no entropy change while the equilibrium method leads to a significant entropy loss.

TABLE 1: Experimental Protonation Energetics of Diols 1−3

M	GB (kJ·mol^{-1})	PA (kJ·mol^{-1})	Δ_pS° (J·mol^{-1}·K^{-1})[a]	method
1	774.3 ± 3.1	817.0 ± 2.9	−34.6 ± 1.0	equilibrium[1]
	770 ± 10			bracketing[2]
		800.2	(3)	kinetic[3]
		801.3	(3)	kinetic[5]
2	826.6 ± 1.7	877.4 ± 2.9	−61.8 ± 4.3	equilibrium[1]
		853.2	(−2)	kinetic[3]
		857.6	(−6)	kinetic[4]
3	855.7 ± 4.5	917.0 ± 6.3	−97.2 ± 5.9	equilibrium[1]
		883.0	(−7)	kinetic[3]
		884.3	(−18)	kinetic[4]

[a] Values obtained by the full entropy analysis method are given in parentheses.

1,3-Propane diol, **2**, has been subjected to three proton-transfer experiments with mesitylene, acetophenone, and styrene by Chen and Stone[1] in the temperature range 500−600 K. Using their experimentally determined ΔS° and ΔH° and the tabulated thermochemistry[14] of the reference bases, we evaluated the GB(**2**), PA(**2**), and Δ_pS°(**2**) indicated in Table 1. The comparison of these values with those obtained by the kinetic method[3,4] shows again a large discrepancy; the deviation in proton affinities attains here more than 20 kJ·mol^{-1}.

Finally, two-proton-transfer equilibrium involving 1,4-butane diol, **3**, and acetophenone or 2-methyl furan were studied by Chen and Stone.[1] Their experiments allow the estimates of GB(**3**), PA(**3**), and Δ_pS°(**3**) presented in Table 1. Again, the proton affinity determined by the kinetic method within the full entropy analysis approach is well below that determined by the equilibrium method; the deviation is now equal to 34 kJ·mol^{-1}.

The clear disagreement observed between the proton affinity values determined from equilibrium constant determination and the kinetic method is disappointing in view of the large use of

the latter procedure to obtain thermochemical data. Such discrepancies are generally attributed to the existence of a reverse activation barrier, which may lead to an underestimate of the proton affinity determination. However, no such barrier seems to be associated with proton-transfer processes even when it involves bidentate bases such as 1,2-ethane diamine[15] or 1,2-ethane diol.[5] Moreover, reverse critical energies as large as 34 kJ·mol^{-1} have not been suspected from the examination of the kinetic energy released during the dissociation of the protonated dimers.[3] The origin of the observed difference remains consequently to be determined. Concerning the protonation entropy, the observation that $\Delta_pS°$ estimated by the kinetic method is far from that determined by the equilibrium method at variable temperature is not surprising. It corroborates other investigations, which demonstrate that indeed the kinetic method (even in its full entropy analysis variant) does not provide the true $\Delta_pS°$ term but only a fraction of it.[3−5] However, the precise understanding of the large $\Delta_pS°$ values revealed by the equilibrium constant determinations is not yet achieved. Clearly, another mean to estimate the proton affinities and the protonation entropies of the diols **1**−**3** to control the origin of these cumulated discrepancies is of interest. This was the goal of our investigation of these three systems by quantum chemical calculations, the results of which are described in the following paragraphs.

Conformational Analysis. As a first approach, a conformational analysis of the neutrals **1**−**3** and their protonated forms **1H**$^+$−**3H**$^+$ has been conducted at the HF/6-31G* level. It allowed us to locate the various minima in the corresponding potential energy surfaces and to estimate the rotational barriers separating the conformers (Table 2). In a second step, each minimum has been reconsidered at the correlated MP2/6-31G* level to identify more safely the lowest-energy conformers (Figures 1−3).

According to previous calculations[2,16] and microwave spectroscopy,[17] the most stable conformation of 1,2 ethane diol, **1**, presents a dihedral angle OCCO close to 60.0° allowing the formation of an intramolecular hydrogen bond (Figure 1). A barrier of 29.8 kJ·mol^{-1} is calculated at HF/6-31G* level for the rotation around the CC bond. It is noteworthy that this value compares within less than 1 kJ·mol^{-1} with the MP2/6-311+G-(2d,p) calculation by Yeh et al.[16] The transition structure is the eclipsed conformation in which the oxygen−oxygen repulsion is at the origin of the corresponding energy barrier. A second minimum has been located at a OCCO angle of 180°; its energy (10.3 kJ·mol^{-1}) may be taken as an estimate of the lower limit of the internal hydrogen-bond energy in **1**. Rotation around one of the two CO bonds passes through a transition structure, situated 16.4 kJ·mol^{-1} above **1**, in which the intramolecular hydrogen bond O**H**···O(*H*) is broken while the (**H**)O···*H*O complementary one begins to be established. To this structural change is associated the constraints because the rotating H is eclipsed with the CH_2OH moiety.

Protonated 1,2-ethane diol, **1H**$^+$, is most stable in a conformation characterized by a dihedral OCCO angle of ∼44° (Figure 1). As discussed previously,[18] this conformation leads to a strong intramolecular hydrogen bond, that is however limited by steric and electrostatic constraints. Accordingly, the O···HO distance in **1H**$^+$ is larger than that calculated for the complex between protonated and neutral methanol, and the intramolecular stabilization energy is well below the stabilization energy of the complex between protonated and neutral methanol. The stabilization afforded by the intramolecular hydrogen bond may be estimated by the energy difference between the most stable conformation of **1H**$^+$ and the anti conformation. The value, 44.8 kJ·mol^{-1} at the HF/6-31G level or 50.0 kJ·mol^{-1} at the MP2/6-31G* level, is clearly less than the 150 kJ·mol^{-1} of stabilization energy calculated for the complex between protonated and neutral methanol.[18,19] The transition structure separating the two localized minima of **1H**$^+$ during the OCCO rotation is an eclipsed conformation with the two CO bonds at 120° and a relative energy of 50.0 kJ·mol^{-1} (HF/6-31G*). Rotation around the C−OH bond needs a considerable critical energy (68.4 kJ·mol^{-1}, CCOH dihedral angle equal to 0°) in keeping with the strong electrostatic repulsion between the hydroxylic hydrogen and the OH_2^+ moiety. Finally, rotation along the C−OH_2^+ bond is accompanied by an intermediate barrier of 32.4 kJ·mol^{-1} (CCOH dihedral angle ∼120°) where the internal hydrogen bond is virtually absent but a favorable electrostatic interaction is preserved.

The most stable conformation of 1,3-propane diol, **2**, is a pseudo-chair structure (Figure 2) in which an intramolecular hydrogen bond is clearly established. Rotation along one or the other CC bond shows two minima at OCCC dihedral angles of ∼60° (the global minimum) and 180° (a conformation less-stable by 9.3 kJ·mol^{-1} because of the breaking of the hydrogen bond). The transition structure separating theses two conformers possesses a relative energy of 22.7 kJ·mol^{-1}. When the rotation along the C−O bonds was considered, it was

TABLE 2: Summary of G2(MP2) Calculations on Neutral and Protonated Diols 1−3[a]

M	E_{tot} (0 K)	$\Delta_fH°_0$	E_{tot} (298 K)	$\Delta_fH°_{298}$[b]
1	−229.893 768	−380.8	−229.887 693	−399.4
1H$^+$	−230.194 555	358.2	−230.188 225	335.3
2	−269.118 886	−395.8	−269.111 692	−419.8
2H$^+$	−269.440 462	288.6	−269.433 227	258.7
3	−308.343 529	−409.6	−308.335 205	−439.6
3H$^+$	−308.676 868	243.9	−308.668 600	208.0

[a] Total energies, E_{tot}, in hartree; heats of formation in kJ·mol^{-1}. [b] Values corrected with the $H°_{298}$ obtained using the hindered rotor model.

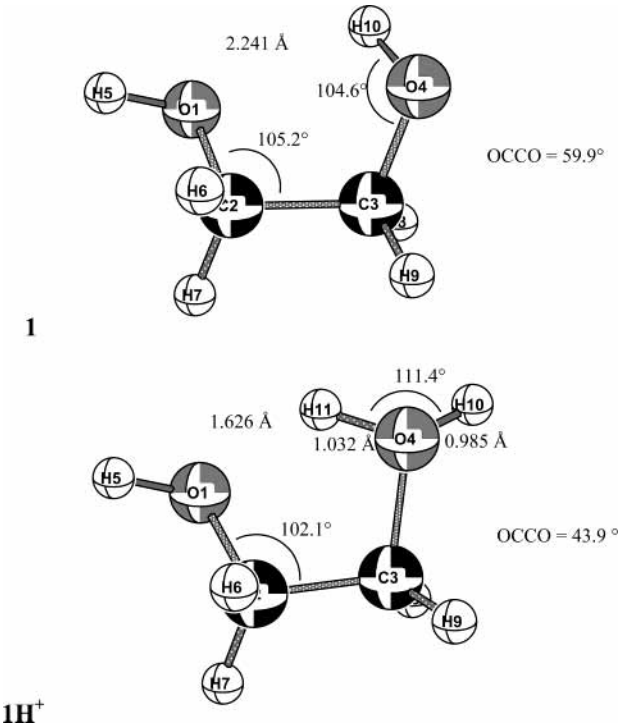

Figure 1. MP2(full)/6-31G* geometries of 1,2-ethane diol, **1**, and its protonated form, **1H**$^+$, in their most stable conformations.

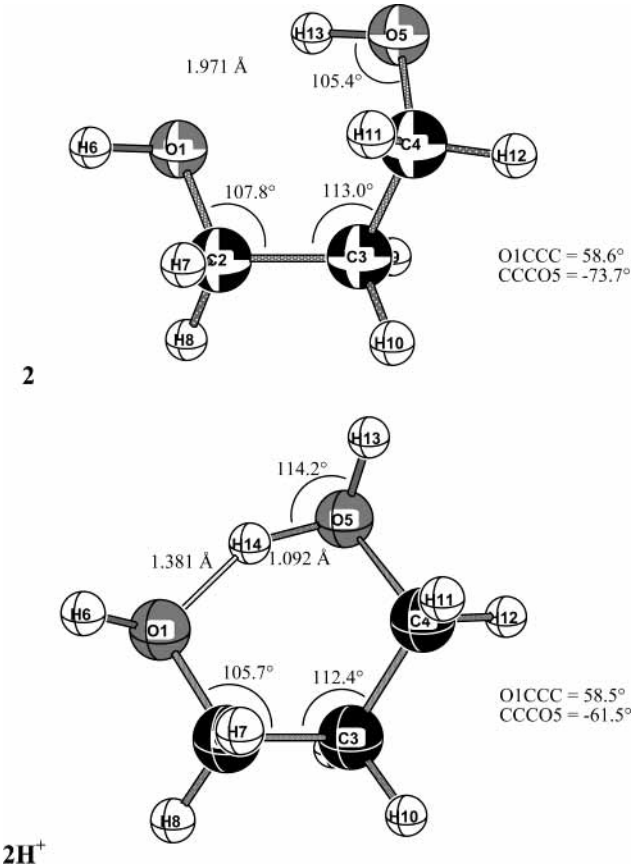

Figure 2. MP2(full)/6-31G* geometries of 1,3-propane diol, **2**, and its protonated form, $\mathbf{2H}^+$, in their most stable conformations.

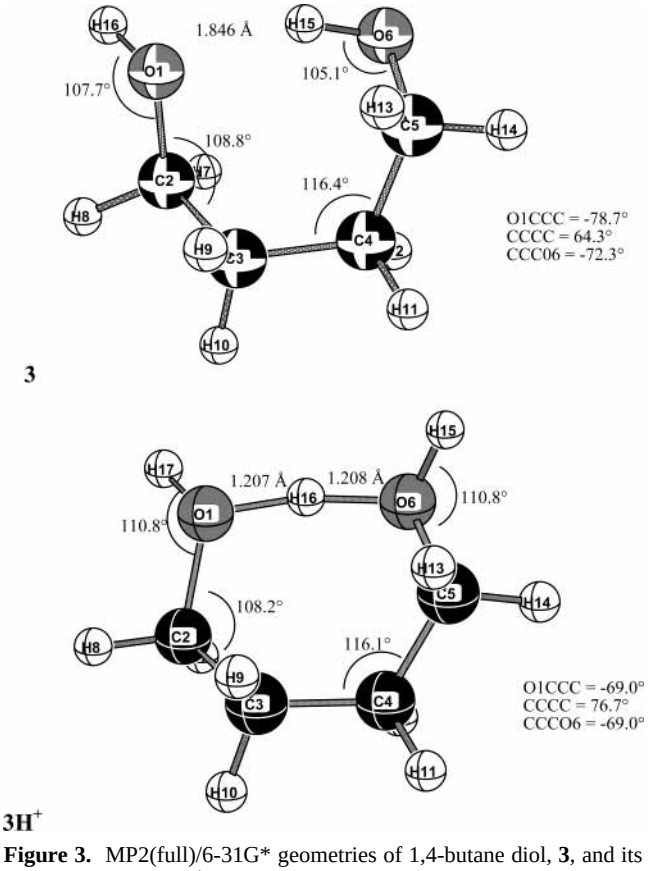

Figure 3. MP2(full)/6-31G* geometries of 1,4-butane diol, **3**, and its protonated form, $\mathbf{3H}^+$, in their most stable conformations.

observed that the highest barrier (situated 11.9 kJ·mol^{-1} above the global minimum) corresponds to the hydrogen-bond inversion O**H**···O(*H*) → (**H**)O···*H*O. Note that this critical energy is slightly less than that calculated for **1**, in agreement with a less-constrained transition structure.

The most stable conformation of the $\mathbf{2H}^+$ ion is also a pseudo-chair structure characterized by the existence of a significant intramolecular hydrogen bond (Figure 2). This is illustrated by the high critical energies associated with the rotations around the CC bonds: 61.8 kJ·mol^{-1} for the C−COH_2^+ rotation and 82.0 for the C−COH rotation. In both cases, the conformations corresponding to a dihedral angle of 180° and the transition structures are very close in structure and in energy. As already noted for protonated 1,2-ethane diol, rotation along the C−OH bond is associated with a higher critical energy; for $\mathbf{2H}^+$, it attains 97.2 kJ·mol^{-1} (for a CCOH dihedral angle of 0°). Rotation of the OH_2^+ group along the CO bond presents a transition structure characterized by a CCOH dihedral angle of 120° and a relative energy of 57.2 kJ·mol^{-1}. Obviously, the increase in rotational barrier height observed for $\mathbf{2H}^+$ with respect to $\mathbf{1H}^+$ is in agreement with the fact that the intramolecular hydrogen bond is higher in the former case than in the latter.

Figure 3 shows 1,4-butane diol, **3**, in its most stable conformation, in which an intramolecular hydrogen bond is established. The second stable conformation, situated 7.4 kJ·mol^{-1} above, is obtained after rotation along the central CC bond, for a dihedral angle of 180°, that is, after breaking the internal hydrogen bond. The barrier separating these two conformers is equal to 14.7 kJ·mol^{-1}. Rotation around the two other CC bonds, which also involves a hydrogen-bond breaking, is associated with a slightly higher barrier of 17.4 kJ·mol^{-1}. Finally, rotation along the C−O bonds is easier because intramolecular hydrogen bonding is preserved most of the time; the critical configuration corresponds to the partner exchange as already noted for the two lower homologues. The corresponding energy barrier is 10.5 kJ·mol^{-1}.

Protonation of **3** gives rise to $\mathbf{3H}^+$ ion strongly stabilized by the intramolecular hydrogen bond (Figure 3). Rotations around one of the three CC bonds always needs a considerable critical energy because it involves the breaking of the hydrogen bond; this explain why the corresponding barriers are as high as 78.8−97.1 kJ·mol^{-1}, that is, values greater than that calculated for $\mathbf{2H}^+$ or $\mathbf{1H}^+$. A comparable result is obtained for the C−OH rotation; the barrier of 119.5 kJ·mol^{-1} is higher than those calculated for $\mathbf{2H}^+$ and $\mathbf{1H}^+$. Concerning the remaining C−OH_2^+ bond, it has been found that the rotation allows the conservation of a significant hydrogen bonding and thus the barrier is markedly reduced with respect to $\mathbf{2H}^+$ (22.6 compared with 57.2 kJ·mol^{-1}).

Protonation Entropies. Molecular third-law entropies, $S°$, were calculated as described in the computational section, that is, by explicitly considering the internal rotations of hindered rotors. The resulting $S°$ values and the details concerning the contributions associated with each rotor are given in Table 2.

Before discussing these results, it is of interest to examine the incidence of the barrier height on the contribution to entropy of the corresponding hindered rotor. Figure 4 shows two extreme cases encountered in the present study. The first rotor is characterized by a small reduced moment of inertia ($I = 0.14 \times 10^{-39}$ g·cm^2); it typically corresponds to a rotation around a C−O(H) bond for the diols **1**−**3**. The second rotor with $I = 10.6 \times 10^{-39}$ g·cm^2 has been chosen to illustrate a rotation around a central C−C bond. As expected, starting with $V_0 = 0$ (the free rotor limit for which $S°$ is calculated using eq 4), the

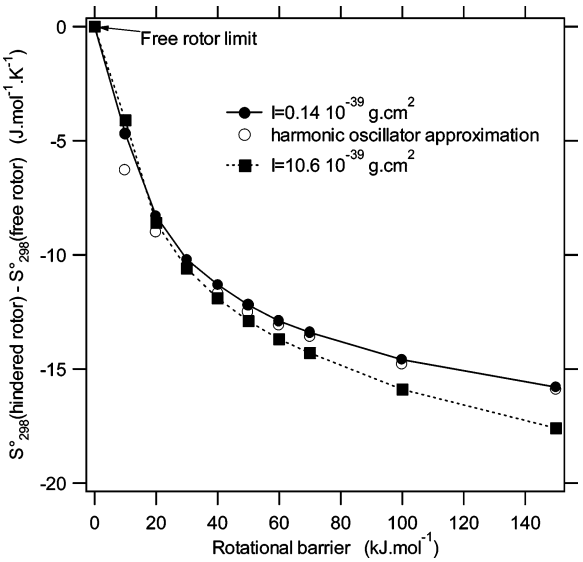

Figure 4. Entropy decrease of two typical hindered rotors as a function of the corresponding rotational barrier.

entropy of the hindered rotor rapidly decreases with increasing V_0. It is interesting to note that, attaining V_0 values of ∼100 kJ·mol^{-1}, that is, the largest barriers calculated for the protonated species **1H**$^+$−**3H**$^+$, the entropy loss is equal to 15 J·mol^{-1}·K^{-1}. In this range of energy barriers, it appears also that the corrections to free rotor $S°$ values are only marginally sensitive to the reduced moment of inertia. When V_0 is less than 100 kJ·mol^{-1}, the two curves in Figure 4 are quasi-superimposable and the $S°$ values do not differ by more than 2 J·mol^{-1}·K^{-1}.

The points corresponding to the harmonic oscillator approximation (eqs 3 and 5) are also reported in Figure 4 for the case $I = 0.14 \times 10^{-39}$ g·cm^2. It appears clearly that this approximation holds correctly in a large part of the explored V_0 domain, particularly for the upper V_0 values, as expected. This comparison is also illustrated by the results given in Table 2. The differences between the $S°$(M) values calculated using the hindered rotor model and those calculated using the harmonic oscillator approximation are 2.4, 3.5, and 6.1 J·mol^{-1}·K^{-1} for M = **1**−**3**, respectively. Concerning the protonated forms, the rotational barriers are so high that the approximation of the harmonic oscillator exactly applies. It should be emphasized, however, that the present calculations employed eq 5 to evaluate the equivalent harmonic frequency. The results are generally different from the values given by Gaussian at the HF/6-31G* level, even with the suggested corrective factors[21]. We observed, on the present system, that the entropy values calculated by Gaussian are situated 6−16% below the estimates based on the harmonic frequencies given by eq 5.

At this stage, indications on the precision of the $S°$ calculated by the hindered rotor model may be given. Possible errors on these estimates may originate from a bad value of the rotational barrier or a crucial change in the reduced moment of inertia during the considered rotation. Concerning the first point, we observed that to produce an increase in $S°$ of 1 J·mol^{-1}·K^{-1}, the decrease in the barrier height should be as high as 20%. Similarly, an increase of I_{red} (see eq 5) by a factor of 2 induces an increase in $S°$ of ∼4 J·mol^{-1}·K^{-1}. Thus, combining these two effects, an error of ±5 J·mol^{-1}·K^{-1} per internal hindered rotation should be expected on $S°$(M). The accuracy of the present entropy estimate can be tested by comparison with results obtained by other means. Seemingly, only the entropy of ethane diol **1** has been experimentally determined; the reported value of 315.5 J·mol^{-1}·K^{-1} has been satisfactorily approached by Yeh et al.[16] with a theoretical value of 312.2 J·mol^{-1}·K^{-1} and is nicely reproduced by our estimate of 314.3 J·mol^{-1}·K^{-1} (Table 2).

TABLE 3: Entropy Calculation at 298 K for the Neutral and Protonated Diols 1−3

species	bond	V_0[a]	$S°$ [b]	$S°_t$[c]	$S°_t$[d]	$S°_t$[e]
1	O1−C2	16.4	314.3	18.7	11.4	10.4
	C2−C3	29.8	(325)	31.2	20.7	20.3
	C3−O4	16.4		18.9	11.6	10.6
1H$^+$	O1−C2	68.4	309.4	18.5	5.0	5.0
	C2−C3	50.0		31.8	19.0	18.7
	C3−O4	32.4		21.8	11.3	10.8
2	O1−C2	11.9	358.7	18.7	12.8	11.7
	C2−C3	22.7	(364)	33.0	23.9	23.3
	C3−C4	22.7		33.0	23.9	23.2
	C4−O5	11.9		18.9	13.0	11.9
2H$^+$	O1−C2	97.2	336.2	18.5	3.4	3.4
	C2−C3	82.0		33.3	17.8	17.8
	C3−C4	61.8		33.8	19.2	19.1
	C4−O5	57.2		22.1	8.9	8.8
3	O1−C2	10.5	405.3	18.7	13.7	12.3
	C2−C3	17.4	(404)	33.5	25.7	24.8
	C3−C4	14.7		36.6	29.6	28.6
	C4−C5	17.4		33.4	25.6	24.7
	C5−O6	10.5		18.9	14.3	12.4
3H$^+$	O1−C2	119.5	373.1	18.6	3.4	3.4
	C2−C3	97.1		33.7	17.9	17.9
	C3−C4	95.5		36.9	21.1	21.1
	C4−C5	78.8		34.2	19.2	19.2
	C5−O6	22.6		22.5	13.5	12.8

[a] Potential energy barrier of the internal rotation around the "bond"; value in kJ·mol^{-1} calculated at the HF/6-31G(d) level. [b] Total entropy (J·mol^{-1}·K^{-1}) of the species considered calculated using the Pitzer's procedure for the torsional modes. Values estimated by the Benson's procedure are given in parentheses.[20] [c] Contribution to the entropy of the torsional modes calculated within the rigid free rotor approximation. [d] Contribution to the entropy of the torsional modes calculated using the Pitzer's method. [e] Contribution to the entropy of the torsional modes calculated within the harmonic oscillator approximation.

For comparison, $S°$(M) values calculated using the Benson's incremental method are also given in Table 2 for **1**−**3**. It is expected that this latter procedure, which does not include the influence of intramolecular hydrogen bonds, would lead to overestimated $S°$ values. This is indeed observed for **1** and **2** but not for **3**.

Heats of Formation and Proton Affinities. The total energies of the most stable structures of **1**−**3** and **1H**$^+$−**3H**$^+$ have been calculated using the composite G2(MP2) method to determine precisely the heat of formation of each species and the corresponding proton affinities. Table 3 gathers the total G2(MP2) energies of **1**−**3** and **1H**$^+$−**3H**$^+$ and the relevant heats of formation calculated using eqs 1 and 2.

Calculated $\Delta_f H°_{298}$(M) (M = **1**−**3**) can be compared with values estimated using the Benson's incremental procedure.[20] The latter method leads to $\Delta_f H°_{298}$(M) = −385, −406, and −426 kJ·mol^{-1} for M = **1**−**3** respectively, that is, a constant amount ∼15 kJ·mol^{-1} above the G2(MP2) results. The difference expected between the two estimates comes from the existence of an intramolecular hydrogen bond, which is not taken into account in the Benson's procedure. Accordingly, as indicated above, the most stable conformations of neutrals **1**−**3** are situated in a limited energy range, ∼8 kJ·mol^{-1} below the conformations in which the intramolecular hydrogen bonds are broken. The G2(MP2) calculated $\Delta_f H°_{298}$(M) thus seems to be satisfactorily evaluated, that is, in the chemical accuracy range of ±5 kJ·mol^{-1}.[6]

TABLE 4: Theoretical Protonation Energetics of Diols 1−3 at 298 K

M	PA[a]	$\Delta_pS°$ [b]	GB[c]
1	795.3	−4.9 (−0.3) ± 15	761.4
2	851.5	−22.5 (−20.2) ± 20	812.4
3	882.4	−32.2 (−29.6) ± 25	840.4

[a] G2(MP2) calculations, kJ·mol^{-1}. [b] $\Delta_pS°(M) = S°(MH^+) - S°(M)$, M = **1**−**3**, J·mol^{-1}·K^{-1}; see Table 3 for the 298 K values of $S°$. Values in parentheses refer to entropies at 600 K. Indicated uncertainties are estimates based on the maximum errors expected in $S°$(M) because of the use of the hindered rotor model (see text). [c] $GB(M) = PA(M) - 298(108.8 - \Delta_pS°(M)) \times 10^{-3}$, kJ·mol^{-1}.

Table 4 summarizes the present computational protonation thermochemistry of molecules **1**−**3**. It first appears that G2(MP2) calculation correctly reproduces the increase in proton affinity experimentally observed from **1** to **3** (Table 1). However, the absolute values of the computed PA(M) are 21.8, 27.1, and 35.5 kJ·mol^{-1} lower than those deduced from equilibrium constant determinations for M = **1**−**3**, respectively. Such deviations are not usual with G2 methods. Interestingly enough, these deviations are considerably reduced when considering the experimental proton affinities determined using the kinetic method in its "full entropy analysis" version. In those cases, the differences in proton affinities are only 5.6, 5.1, and 2.1 kJ·mol^{-1} for M = **1**−**3**, respectively, that is, more in line with the expected accuracy of the G2 method.

Second, the entropy loss expected to be associated with protonation is confirmed by the calculation. Moreover, the increasing absolute value of $\Delta_pS°$(M), expected when the size of the diol increases, is also reflected by the results given in Table 4. Note that the use of the $S°$ calculated by Gaussian using the scaled HF/6-31G* vibrational frequencies leads to $\Delta_pS°$ of 2.9, −1.6, and −3.5 J·mol^{-1}·K^{-1}, respectively, that is, values that do not reflect any significant protonation entropy loss. This large discrepancy is mainly due to the wrong estimate of the low frequencies which, in the present cases, underestimate severely the calculated $S°$ of the neutral molecules as mentioned above. However, the most prominent observation is that the calculated protonation entropies $\Delta_pS°$(M) (Table 4) are systematically of lower magnitude than those determined from variable temperature equilibrium experiments[1] (Table 1). Because experiments have been done in a 500−600 K source temperature range,[1] we indicate also the $\Delta_pS°$(M) values calculated at 600 K. Under these circumstances, the differences between calculated and experimental $\Delta_pS°$(M) values are equal to 34, 42, and 68 J·mol^{-1}·K^{-1} for M = **1**−**3**, respectively. What is surprising is the fact that the $\Delta_pS°$(M) values by Chen and Stone[1] are lower than the expected minimum $\Delta_pS°$(M), which can be estimated by assuming that all of the internal rotors are free in the neutral molecules M and hindered in their protonated forms MH^+. Accordingly, in this hypothesis $\Delta_pS°$(M) should be equal to −30, −52, and −64 J·mol^{-1}·K^{-1} for M = **1**−**3**, respectively. Clearly, the experimental values are beyond these lower limits.

Combining now the G2(MP2) proton affinities and the protonation entropies $\Delta_pS°$(M) computed in the frame of the hindered rotor model, we calculate the estimate of the gas-phase basicities, GB(M), indicated in Table 4, for molecules **1**−**3**. In keeping with the above observations, the calculated quantities disagree with the values deduced from proton-transfer equilibrium measurements at variable temperature. By comparison with the experimental determination by Chen and Stone,[1] a difference of ∼15 kJ·mol^{-1} in the GB values is observed. It may be pointed out that, with respect to proton affinities, the difference between the theoretical and experimental quantities is less-pronounced. This illustrates a compensation effect between the proton affinities and the $T\Delta S°$ term, which reduces the discrepancy to a constant deviation of ∼15 kJ·mol^{-1} on the GB values.

Conclusion

The theoretical results presented in this study used state of the art computational techniques: G2(MP2) method, expected to provide proton affinities with an accuracy of ca. ±5 kJ·mol^{-1}, and consideration of hindered rotor constraints in the calculation of molecular entropy. The latter is expected to give $\Delta_pS°$(M) values within ±6−10 J·mol^{-1}·K^{-1}. The results show considerable differences with figures obtained from equilibrium constant determination at variable temperature.[1] Computed proton affinities are 22−35 kJ·mol^{-1} lower than the values obtained by Chen and Stone.[1] Similarly, differences in $\Delta_pS°$(M) attain 34−68 J·mol^{-1}·K^{-1}. When considering the gas-phase basicities, the deviation is reduced to "only" 15 kJ·mol^{-1}. The origin of the discrepancies is delicate to be firmly identified. Maybe these differences originate from experimental difficulties (such as, true temperature and pressure measurement and existence of competitive dissociation or association processes) or from inadequacy of the present theoretical treatment. The good agreement observed between computed and experimentally determined proton affinities, if the latter is determined by the kinetic method,[3,4] is indeed in favor of the first hypothesis. However, the present data more reasonably suggest to explore again this system to clarify the origin of the observed discrepancies.

Acknowledgment. We gratefully acknowledge Dr. Bonnie McBride for providing us the PAC99 computer program and for his help during its installation on our computer station.

Supporting Information Available: Detailed geometries and vibrational frequencies used in the present work. This material is available free of charge via the Internet at http://pubs.acs.org.

References and Notes

(1) Chen, Q.-F.; Stone, J. A. *J. Phys. Chem. A* **1995**, *99*, 1442.

(2) Bouchoux, G.; Jezequel, S.; Penaud-Berruyer, F. *Org. Mass Spectrom*. **1993**, *28*, 421.

(3) Bouchoux, G.; Djazi, F.; Gaillard, F.; Vierezet, D. *Int. J. Mass Spectrom*. **2003**, *227*, 479.

(4) Bouchoux, G.; Buisson, D.-A.; Bourcier, S.; Sablier, M. *Int. J. Mass Spectrom*., in press.

(5) Bouchoux, G.; Buisson, D.-A.; Sablier, M.; Berruyer-Penaud, F., manuscript in preparation.

(6) Curtiss, L. A.; Raghavachari, K.; Redfern, P. C.; Pople, J. A. *J. Chem. Phys*. **1997**, *106*, 1063.

(7) (a) East, A. L. L.; Radom, L. *J. Chem. Phys*. **1997**, *106*, 6655. (b) East, A. L. L.; Smith, B. J.; Radom, L. *J. Am. Chem. Soc*. **1997**, *119*, 9014.

(8) Bouchoux, G.; Choret, N.; Berruyer-Penaud, F. *J. Phys. Chem. A* **2001**, *105*, 3989.

(9) Bouchoux, G.; Choret, N.; Berruyer-Penaud, F.; Flammang, R. *Int. J. Mass Spectrom*. **2002**, *217*, 195.

(10) Frisch, M. J.; Trucks, G. W.; Schlegel, H. B.; Scuseria, G. E.; Robb, M. A.; Cheeseman, J. R.; Zakrzewski, V. G.; Montgomery, J. A., Jr.; Stratmann, R. E.; Burant, J. C.; Dapprich, S.; Millam, J. M.; Daniels, A. D.; Kudin, K. N.; Strain, M. C.; Farkas, O.; Tomasi, J.; Barone, V.; Cossi, M.; Cammi, R.; Mennucci, B.; Pomelli, C.; Adamo, C.; Clifford, S.; Ochterski, J.; Petersson, G. A.; Ayala, P. Y.; Cui, Q.; Morokuma, K.; Malick, D. K.; Rabuck, A. D.; Raghavachari, K.; Foresman, J. B.; Cioslowski, J.; Ortiz, J. V.; Stefanov, B. B.; Liu, G.; Liashenko, A.; Piskorz, P.; Komaromi, I.; Gomperts, R.; Martin, R. L.; Fox, D. J.; Keith, T.; Al-Laham, M. A.; Peng, C. Y.; Nanayakkara, A.; Gonzalez, C.; Challacombe, M.; Gill, P. M. W.; Johnson, B. G.; Chen, W.; Wong, M. W.; Andres, J. L.; Head-Gordon, M.; Replogle, E. S.; Pople, J. A. *Gaussian 98*, revision A.6; Gaussian, Inc.: Pittsburgh, PA, 1998.

(11) Nicolaides, A.; Rauk, A.; Glukhovtsev, M. N.; Radom, L. *J. Phys. Chem*. **1996**, *100*, 17460.

(12) McBride, B. J.; Gordon, S. *PAC99. Computer Program for Calculating and Fitting Thermodynamic Functions*; RP1271; NASA: 1992.
(13) Pitzer, K. S.; Gwinn, W. D. *J. Chem. Phys.* **1942**, *10*, 428.
(14) Hunter, E. P. L.; Lias, S. G. *J. Phys. Chem. Ref. Data* **1988**, *27*, 413.
(15) Wang, Z.; Chu, I. K.; Rodrigez, C. F.; Hopkinson, A. C.; Siu, K. K. M. *J. Phys. Chem. A* **1999**, *103*, 8700.
(16) Yeh, T. S.; Chang, Y. P.; Su, T. M.; Chao, I. *J. Phys. Chem*. **1994**, *98*, 8921 and references therein.
(17) Vasquez, S. A.; Rios, M. A.; Caballeira, L. *J. Comput. Chem.* **1992**, *13*, 851.
(18) Bouchoux, G.; Choret, N.; Flammang, R. *J. Phys. Chem. A* **1997**, *101*, 4271.
(19) Bouchoux, G.; Choret, N. *Rapid Commun. Mass Spectrom*. **1997**, *11*, 1799.
(20) Benson, S. W. *Thermochemical kinetics*, 2nd ed.; Wiley Int.: New York, 1976.
(21) Scott, A. P.; Radom, L. *J. Phys. Chem.* **1996**, *100*, 16502.